Characterisation of labelled Csp*Tm* and polyproline

Labelling specificity. Trypsin digests of the doubly labelled protein in combination with mass spectrometry did not identify any labelled fragments apart from the terminal ones, indicating specific labelling of the cysteines. Furthermore, no triply labelled protein was detectable. The two possible labelling permutants were separated by ion exchange chromatography. In the preparation used, the ratio of C-terminal Alexa 488 (A-CspTm-D) to Alexa 594 (D-CspTm-A) was about 3 to 1. A comparison of single molecule measurements on the two permutants yielded widths for the transfer efficiency distributions of the unfolded state that are identical within experimental error, and the mean values differed by about 0.04. The contribution of 25% D-CspTm-A present in our preparation of A-CspTm-D therefore has a negligible effect on the width.

Photophysical properties of the conjugated dyes. The quantum yield of Alexa 488 attached to the native protein is about 25% lower (0.40) than if attached to poly-Pro (0.53), probably due to interactions with the protein surface, leading to fluorescence quenching. However, our results focus on the properties of the protein in the unfolded state, where a well-defined local environment is not present. Correspondingly, the quantum yields of Alexa 488 attached to poly-Pro and Csp*Tm* are equal (0.52 ± 0.05) at GdmCl concentrations beyond the unfolding transition of the protein. In the case of the acceptor, Alexa 594, the quantum yields are identical for labelled polyproline and Csp*Tm* over the entire range of GdmCl concentrations. The only significant difference is the lower extinction coefficient of Alexa 594 succinimidyl ester (used for labelling polyproline) compared to the maleimide (used for labelling the protein), corresponding to a 3% lower value for the Förster distance R_0. This small offset does not have any effect on our conclusions. Evidence for the similarity of the conformational freedom of the dyes attached to poly-Pro and Csp*Tm* comes from their small residual steady state polarization anisotropy (between 0.03 and 0.09), which indicates that the dyes almost completely sample the distribution of relative orientations in less than the donor fluorescence lifetime of about 1 ns.[4] Complete averaging during the fluorescence lifetime of distance fluctuations due only to the dyes precludes any contribution to the measured width of the transfer efficiency distributions from such fluctuations.

Ensemble folding characteristics of labelled Csp*Tm*. Labelling of Csp*Tm* with Alexa 488 and Alexa 594 maleimide at the recombinantly introduced cysteine residues results in a shift of the denaturation midpoint from 2.5 M GdmCl to 2.0 M GdmCl. In spite of this slight destabilization, the folding properties characteristic of this family of small cold shock proteins are conserved. Both the agreement of the thermodynamic parameters derived from the equilibrium unfolding curve (Figure 3) and the stopped-flow measurements (Figure S1), and the linearity of the denaturant dependencies of the folding and unfolding rate constants in the chevron plot (Figure S1) indicate good agreement with a two-state model. The high α-value of 0.94 calculated from the slopes in the chevron plot is typical for the native-like transition states generally observed in small cold shock proteins. From these data we conclude that the dye labelling used here does not alter the folding mechanism of the protein.

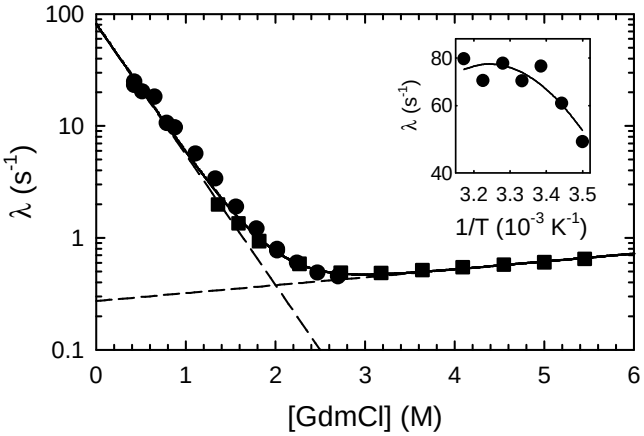

Figure S1. Denaturant and temperature dependence of the folding kinetics of labelled Csp*Tm*. The solid line is a joint fit to the observed rate constants λ under folding (circles) and unfolding (squares) conditions. The dashed lines are the denaturant dependencies of the folding and unfolding rate constants derived from the fit. The inset shows the dependence of the extrapolated folding rate constant on temperature T in the absence of denaturant, corrected for the change of solvent viscosity η with T, assuming $\lambda \propto \eta^{-1}$.[32,33] To determine the activation enthalpy for folding $\Delta H^{\ddagger}$ at room temperature T_0, the data were fit (solid line) to the equation

$$k_f = A \exp\left\{-\frac{1}{RT}\left[\Delta H^{\ddagger}(T_0) + \Delta c_p^{\ddagger}\cdot\left((T-T_0) - T\ln\frac{T}{T_0}\right)\right]\right\},$$

where $\Delta c_p^{\ddagger}$ is the difference in heat capacity (assumed to be independent of temperature in this derivation) between the unfolded state and the transition state, and A is a freely adjustable parameter. The values obtained were $\Delta H^{\ddagger}(T_0)$ = 12 kJ mol^{-1}, $\Delta c_p^{\ddagger}$ = -1.1 kJ mol^{-1} K^{-1} and A = 7.8 kHz. Data were collected by observing the change in donor fluorescence in an Advanced Photophysics stopped-flow spectrometer SX-18MV using an excitation wavelength of 450 nm.

Distribution functions and calculation of radii of gyration

For a gaussian chain, the radial probability distribution is

$$P(r) = 4\pi r^2 \left(\frac{3}{2\pi \left\langle r^2 \right\rangle} \right)^{3/2} \exp\left(-\frac{3r^2}{2\left\langle r^2 \right\rangle} \right), \qquad (2)$$

where r is the end-to-end distance. With $\left\langle r^2 \right\rangle^{1/2} = R_0$ = 5.4 nm and $E(r) = 1/(1+(r/R_0)^6)$, equation (2) can be transformed into the equilibrium distribution shown in Figure 4a using

$$P(E) = P(r)\left|\frac{dr}{dE}\right|. \qquad (3)$$

In the fast reconfiguration limit (Figure 4b), the mean value of the FRET efficiency for the unfolded molecules is given by:

$$\left\langle E_U \right\rangle = \int_0^\infty E(r)\, P(r)\, dr. \qquad (4)$$

The mean squared end-to-end distance and radius of gyration of a gaussian chain are related by[34]

$$\langle R_g^2 \rangle = \langle r^2 \rangle / 6. \qquad (5)$$

At 6 M GdmCl, $\langle E_U \rangle \approx 0.43$ yields $\langle R_g \rangle \approx 2.8$ nm, in good agreement with $\langle R_g \rangle \approx 2.5$ nm obtained from an empirical curve for a series of unfolded proteins of different lengths measured by ensemble methods[13] (including an additional 4 residues to account for the dyes and linkers). In the absence of denaturant, $\langle E_U \rangle \approx 0.7$ (Figure 3) corresponds to an $\langle R_g \rangle$ of about 1.9 nm (the R_g of the native structure[30] is 1.1 nm). In calculations by Shea and Brooks[28], the values of $\langle R_g \rangle$ determined for the unfolded molecules both above (~1.8 nm) and at the folding temperature (~1.4 nm) are smaller than the values calculated from the mean FRET efficiencies above (2.7 nm, after subtracting the dye contribution) and at (2.3 nm) the midpoint denaturant concentration in our experiments; an $\langle R_g \rangle$ of 1.4 nm would correspond to $\langle E_U \rangle \approx$ 0.9, indistinguishable from the folded protein (Fig. 2).

32. Jacob, M. & Schmid, F. X. (1999) Protein folding as a diffusional process. *Biochemistry. 38*, 13773-9.

33. Jas, G. S., Eaton, W. A. & Hofrichter, J. (2001) Effect of viscosity on the kinetics of α-helix and β-hairpin formation. *Journal of Physical Chemistry B. 105*, 261-272.

34. Cantor, C. R. & Schimmel, P. R. *Biophysical Chemistry, Part III. The Behavior of Biological Macromolecules* (W. H. Freeman, New York, 1980).